Progress In Electromagnetics Research, Vol. 134, 47–62, 2013

A NOVEL COMPACT DUAL-FREQUENCY COUPLED-LINE TRANSFORMER WITH SIMPLE ANALYTICAL DESIGN EQUATIONS FOR FREQUENCY-DEPENDENT COMPLEX LOAD IMPEDANCE

Yongle Wu[1, 2, 3, *], Weinong Sun[3], Sai-Wing Leung[3], Yinliang Diao[3], and Kwok-Hung Chan[4]

[1]School of Electronic Engineering, Beijing University of Posts and Telecommunications, Beijing, China

[2]State Key Laboratory of Millimeter Waves, Nanjing 210096, China

[3]Department of Electronic Engineering, City University of Hong Kong, Hong Kong, China

[4]Department of Computer Science and Engineering, Nagoya Institute of Technology, Japan

Abstract—In order to perfectly match arbitrary frequency-dependent complex load impedances at two uncorrelated frequencies, a novel coupled-line impedance transformer without transmission-line stubs is proposed in this paper. This transformer mainly features small size, wide bandwidth, simple analytical design method, and easy planar implementation. The transformer simply consists of a coupled-line section and an additional transmission-line section. Due to the usage of a coupled-line section, the theoretical synthesis of the proposed transformer becomes very simple when compared with previous transformers and the total size of the planar circuit without deterioration of operating bandwidth becomes small. Furthermore, several numerical examples are presented to demonstrate the flexible dual-frequency matching performance. Finally, the profile of matching frequency-dependent complex load impedance at two arbitrary frequencies has been examined by simulation and measurement of two microstrip generalized T-junction power dividers. Good agreement between the calculated results and measured ones justifies this proposed transformer and the design theory.

Received 19 October 2012, Accepted 12 November 2012, Scheduled 14 November 2012

* Corresponding author: Yongle Wu (wuyongle138@gmail.com).

1. INTRODUCTION

Impedance transformers, namely, matching networks are important and fundamental circuit cells in several microwave components (devices) and systems [1–6]. For example, impedance transformers are main parts of various power dividers and combiners. In addition, impedance transformers can be frequently applied in advanced antenna arrays and power amplifiers. The conventional implementation methods of impedance transformers include using lumped components (such as inductors and capacitors), distributed components (such as microstrip and stripline), and their combinations. Therefore, finding appropriate impedance transformers is one of the important works in the antennas and power amplifiers design.

The well-known impedance transformer is the quarter-wavelength transmission line. However, it is obvious that this kind of impedance transformer cannot satisfy the requirement of arbitrary dual-band operations. By applying the conventional transmission-line implementation methods, various kinds of dual-band impedance transformers have been investigated in [7–12]. To match with two different real-value resistances, a set of small dual-frequency transformer with analytical design equations have been developed in [7]. The complex terminated impedance case of dual-band impedance transformers has been first discussed in [8]; however, the design equations are not analytical, requiring a complicated analysis process. Similar mathematical-solving synthesis difficulties in the design of dual-band impedance transformers discussed in [9, 10] still exist. Although the closed-form design equations for generalized impedance transformers are given in [11] and the rigorous dual-frequency matching for frequency-dependent complex load impedance is satisfied, the mathematical expressions are also complex. Obviously, the design process of [11] is quite difficult to repeat due to complex equations. In addition, applying open-/short-circuited transmission-line stubs into dual-band impedance transformers [12] directly results in narrow operating bandwidth and a large-sized circuit layout.

The implementation method for impedance transformer by using coupled transmission lines has also attracted the attention of many researchers [13–15]. In [13], a broad-band quarter-wavelength impedance transformer has been proposed. The required even- and odd-mode impedance of coupled lines cannot be easily realized in microstrip technology. In [14], a novel coupled-line impedance transformer has been developed. This impedance transformer can match real and complex loads in both narrow and wide frequency bands. However, the dual-band application is not considered. By

using an asymmetric broadside coupled line, a small-size impedance transformer is provided in [15]. Note that only single-band application has been studied.

Because dual-band RF systems and components in [16–19] become very significant in satisfying both the multi-standard software defined radios and the fast evolution of wireless communication standards, developing new and simple design approaches to dual-band transformers for frequency-dependent complex load impedance becomes imperative. In order to achieve this goal, a novel dual-frequency coupled-line impedance transformer with a closed-form design approach and practical examples for frequency-dependent complex load impedance is proposed in this paper. This transformer configuration consists of a coupled-line section and a transmission line. It has compact size and reliable analytical design approach. The proposed transformer can be easily applied in the printed circuit board (PCB)-based dual-band passive circuit and power amplifiers. It is worth mentioning that one of its attractive attributes is the provided design method, which is based on simple closed-form mathematical expressions. Additionally, two generalized T-junction power dividers with different power-dividing coefficients at two arbitrary operating frequencies are constructed, designed, fabricated, and measured. The measured results agree well with the calculated ones.

2. THE PROPOSED CIRCUIT AND DESIGN APPROACH

Figure 1 shows the circuit configuration of the proposed impedance transformer. This transformer includes two parts: 1) a section coupled

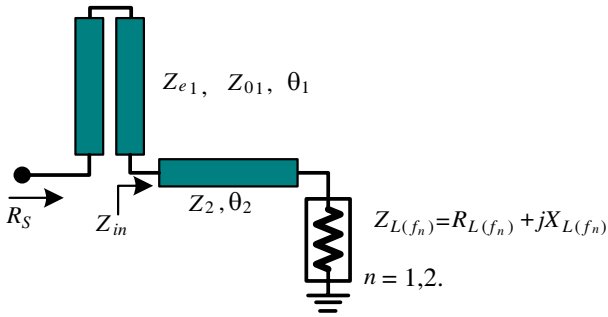

Figure 1. The proposed dual-band coupled-line impedance transformer for arbitrary complex frequency-dependent terminated impedances.

line; 2) a single-section traditional transmission line. The even-mode (odd-mode) characteristic impedance for the coupled-line section is $Z_{e1}(Z_{o1})$ and its electrical length is θ_1. The characteristic impedance of the traditional transmission line is Z_2 and its electrical length is θ_2. As shown in Figure 1, the source resistance is R_S which is usually equal to $50\,\Omega$. However, the required matched load impedance is complex and frequency dependent. For arbitrary dual-frequency application, namely f_1 and $f_2(f_2 \geq f_1)$, these terminated load impedances are $Z_{L(f_1)} = R_{L(f_1)} + jX_{L(f_1)}$ at f_1 and $Z_{L(f_2)} = R_{L(f_2)} + jX_{L(f_2)}$ at f_2, respectively. The values of four parameters such as $R_{L(f_1)}$, $R_{L(f_2)}$, $X_{L(f_1)}$, and $X_{L(f_2)}$ are arbitrary, indicating most cases of the terminated impedances. The ABCD matrix of the coupled-line section can be derived from scattering parameters in [20] as

$$\begin{cases} A_1 = D_1 = \dfrac{Z_{e1} - Z_{o1}\tan^2(\theta_1)}{Z_{e1} + Z_{o1}\tan^2(\theta_1)}, \\ B_1 = \dfrac{2Z_{e1}Z_{o1}j\tan(\theta_1)}{Z_{e1} + Z_{o1}\tan^2(\theta_1)}, \\ C_1 = \dfrac{2j\tan(\theta_1)}{Z_{e1} + Z_{o1}\tan^2(\theta_1)}. \end{cases} \tag{1}$$

Furthermore, the input impedance Z_{in} presented in Figure 1 can be defined as

$$Z_{in} = R_{in} + jX_{in}. \tag{2}$$

According to transmission-line theory and dual-frequency matching results [9, 11], the values of the characteristic impedance Z_2 and electrical length θ_2 at the first operating frequency f_1 of the transmission-line section shown in Figure 1 can be expressed by

$$Z_2 = \sqrt{\begin{array}{l} R_{L(f_1)}R_{L(f_2)} + X_{L(f_1)}X_{L(f_2)} \\ + \frac{[X_{L(f_1)}+X_{L(f_2)}][R_{L(f_1)}X_{L(f_2)}-X_{L(f_1)}R_{L(f_2)}]}{R_{L(f_2)}-R_{L(f_1)}} \end{array}}, \tag{3}$$

$$\theta_{2(f_1)} = \frac{n\pi + \arctan\left[\frac{Z_2(R_{L(f_1)}-R_{L(f_2)})}{R_{L(f_1)}X_{L(f_2)}-X_{L(f_1)}R_{L(f_2)}}\right]}{1+p}, \tag{4}$$

where $p = f_2/f_1$ and is frequency-ratio coefficient, and n is an arbitrary positive integral or equal to zero. If the design parameters for the transmission line are known, the internal defined parameter, input impedance Z_{in} at the first frequency f_1, can be calculated by

$$(R_{in(f_1)}+jX_{in(f_1)}) = \frac{Z_2[R_{L(f_1)}+jX_{L(f_1)}+jZ_2\tan(\theta_{2(f_1)})]}{Z_2 - X_{L(f_1)}\tan(\theta_{2(f_1)}) + jR_{L(f_1)}\tan(\theta_{2(f_1)})}. \tag{5}$$

It is necessary to point out that the input impedance Z_{in} at the second frequency f_2 has the following equation associated with (5):

$$R_{in(f_2)} + jX_{in(f_2)} = \mathrm{con}j(R_{in(f_1)} + jX_{in(f_1)}), \tag{6}$$

where $\mathrm{con}j(\bullet)$ is a complex conjugate function.

Then, the coupled-line section can be used to match the input impedance Z_{in} to the source resistance R_S at both f_1 and f_2. The following relationship can be obtained as

$$R_S = \frac{A_{1(f_1)}(R_{in(f_1)} + jX_{in(f_1)}) + B_{1(f_1)}}{C_{1(f_1)}(R_{in(f_1)} + jX_{in(f_1)}) + D_{1(f_1)}}. \tag{7a}$$

$$R_S = \frac{A_{1(f_2)}(R_{in(f_2)} + jX_{in(f_2)}) + B_{1(f_2)}}{C_{1(f_2)}(R_{in(f_2)} + jX_{in(f_2)}) + D_{1(f_2)}}. \tag{7b}$$

After combining (1) and (7), the following equations can be derived as

$$\begin{cases} 2X_{in(f_1)}R_S\tan(\theta_{1(f_1)}) = (R_S - R_{in(f_1)})\left[Z_{e1} - Z_{o1}\tan^2\left(\theta_{1(f_1)}\right)\right] \\ 2(R_{in(f_1)}R_S - Z_{e1}Z_{o1})\tan(\theta_{1(f_1)}) = X_{in(f_1)}\left[Z_{e1} - Z_{o1}\tan^2\left(\theta_{1(f_1)}\right)\right] \end{cases}. \tag{8}$$

By solving Equation (8) at two different operating frequencies f_1 and f_2, we can obtain a group of simple and analytical design equations for the even- and odd-mode characteristic impedances, which is

$$Z_{o1} = \frac{-\frac{2(X_{in(f_1)})R_S\tan(\theta_{1(f_1)})}{(R_S - R_{in(f_1)})} \pm \sqrt{\left[\frac{2(X_{in(f_1)})R_S\tan(\theta_{1(f_1)})}{(R_S - R_{in(f_1)})}\right]^2 - 4\tan^2(\theta_{1(f_1)})\left[\frac{(X_{in(f_1)})^2R_S}{(R_S - R_{in(f_1)})} - R_{in(f_1)}R_S\right]}}{2\tan^2(\theta_{1(f_1)})}, \tag{9}$$

$$Z_{e1} = \frac{2X_{in(f_1)}R_S\tan(\theta_{1(f_1)})}{(R_S - R_{in(f_1)})} + Z_{o1}\tan^2(\theta_{1(f_1)}), \tag{10}$$

where the electrical length $\theta_{1(f_1)}$ is determined by

$$\theta_{1(f_1)} = \frac{\pi}{1+p}. \tag{11}$$

Note that the value of n in (4) and the sign of "$\pm$" in (9) should be chosen manually according to the practical requirements.

The main design procedure of this impedance transformer can be summarized as follows.

1) According to the given two frequencies f_1 and f_2 practical applications, the values of frequency-dependent load impedances $Z_{L(f_1)} = R_{L(f_1)} + jX_{L(f_1)}$ and $Z_{L(f_2)} = R_{L(f_2)} + jX_{L(f_2)}$ are known.

2) The electrical length $\theta_{1(f_1)}$ of the uncoupled transmission line can be determined by (11) while the electrical length $\theta_{2(f_1)}$ of the coupled-line section can be calculated by (4). Note that there are simple relationships between electrical lengths operating at f_1 and f_2, which are $\theta_{1(f_2)} = p\theta_{1(f_1)}$ and $\theta_{2(f_2)} = p\theta_{2(f_1)}$.

3) The characteristic impedance Z_2 can be obtained by (3) while the internal parameter, namely, input impedance $R_{in(f_1)} + jX_{in(f_1)}$, is determined by (5).

4) Once the source resistance R_S is known (for example, $R_S = 50\,\Omega$), the odd- and even-mode characteristic impedances Z_{o1} and Z_{e1} can be calculated using (9) and (10).

3. NUMERICAL EXAMPLES

In order to illustrate the flexibility of the dual-frequency matching capability for this proposed impedance transformer, three groups of numerical examples are presented when the source resistance satisfies $R_S = 50\,\Omega$. The real and imaginary parts of the frequency-dependent load impedance are plotted in Figure 2. The first group of examples include four different cases which are cases A1–A4. The initial required design parameters are listed in Table 1. According to the provided analytical design formula in Section 2, the calculated circuit parameters are obtained as given in Table 2. Figure 3 shows the theoretical responses of these four cases. In cases A1–A4, the first frequency f_1 is fixed as 1 GHz but the second frequency f_2 varies from 1.8 to 2.2 GHz. The perfect flexible dual-band matching can be observed in Figure 3. Different from the cases A1–A4, another group of numerical examples including cases B1–B4 is designed for varying the first frequency f_1. The initial and designed circuit parameters are listed in Tables 3 and 4, respectively. The input-port scattering parameters of cases B1–B4 are shown in Figure 4. As shown in Figure 4, the first matching frequency f_1 varies from 1.4 to 1.7 GHz while the second matching

Table 1. The initial known design parameters for design requirements in cases A1–A4.

Cases	f_1 (GHz)	f_2 (GHz)	$Z_{L(f_1)}$ (Ω)	$Z_{L(f_2)}$ (Ω)	n
Case A1	1	1.8	$80 + j14.4$	$84.7109 + j18.2678$	1
Case A2	1	1.9	$80 + j14.4$	$85.3496 + j18.9461$	1
Case A3	1	2	$80 + j14.4$	$86 + j19.68$	1
Case A4	1	2.2	$80 + j14.4$	$87.3369 + j21.3334$	1

Table 2. The calculated circuit parameters based on the proposed analytical approach for cases A1–A4.

Cases	Z_{e1} (Ω)	Z_{o1} (Ω)	θ_1 (Degree) at f_1	Z_2 (Ω)	θ_2 (Degree) at f_1
Case A1	129.2	43.95	64.3	93.4	42.4
Case A2	115.6	49.55	62.1	94.3	41.2
Case A3	104.7	55.23	60	95.2	40.2
Case A4	88.1	66.92	56.3	97.4	38.2

Table 3. The initial known design parameters for design requirements in cases B1–B4.

Cases	f_1 (GHz)	f_2 (GHz)	$Z_{L(f_1)}$ (Ω)	$Z_{L(f_2)}$ (Ω)	n
Case B1	1.4	3	$82.2696 + j16.0315$	$93.2000 + j31.2960$	1
Case B2	1.5	3	$82.8634 + j16.5263$	$93.2000 + j31.2960$	1
Case B3	1.6	3	$83.4680 + j17.0617$	$93.2000 + j31.2960$	1
Case B4	1.7	3	$84.0838 + j17.6410$	$93.2000 + j31.2960$	1

frequency f_2 is fixed as 3 GHz. The dual-band matching performance for cases B1–B4 is perfect in Figure 4. Note that cases A1–A4 and B1–B4 have good dual-frequency matching performance when one of the operating frequencies is fixed. In the third group of numerical examples, namely, cases C1–C4, both the first frequency f_1 and f_2 vary. The initial and designed circuit parameters are listed in Tables 5 and 6, respectively. Figure 5 presents the theoretical reflection coefficient responses. Similarly, the flexible dual-frequency matching performance for cases C1–C4 is obvious in Figure 5.

4. FABRICATED MICROSTRIP POWER DIVIDERS USING THE PROPOSED IMPEDANCE TRANSFORMERS

From a practical point of view, this proposed coupled-line impedance transformers can be easily applied in the design of dual-band power

Table 4. The calculated circuit parameters based on the proposed analytical approach for cases B1–B4.

Cases	Z_{e1} (Ω)	Z_{o1} (Ω)	θ_1 (Degree) at f_1	Z_2 (Ω)	θ_2 (Degree) at f_1
Case B1	97.4	75.9	57.3	113.3	41.7
Case B2	112.4	67.7	60	114.5	43.9
Case B3	129.6	60.3	62.6	115.7	46.0
Case B4	149.8	53.6	65.1	117.0	48.0

Table 5. The initial known design parameters for design requirements in cases C1–C4.

Cases	f_1 (GHz)	f_2 (GHz)	$Z_{L(f_1)}$ (Ω)	$Z_{L(f_2)}$ (Ω)	n
Case C1	1.3	2	$81.6866 + j15.5742$	$86 + j19.6800$	1
Case C2	1.2	2.1	$81.1141 + j15.1515$	$86.6624 + j20.4741$	1
Case C3	1.1	2.2	$80.5520 + j14.7610$	$87.3369 + j21.3334$	1
Case C4	1	2.3	$80 + j14.4000$	$88.0239 + j22.2632$	1

Table 6. The calculated circuit parameters based on the proposed analytical approach for cases C1–C4.

Cases	Z_{e1} (Ω)	Z_{o1} (Ω)	θ_1 (Degree) at f_1	Z_2 (Ω)	θ_2 (Degree) at f_1
Case C1	193.8	31.6	70.9	97.6	48.3
Case C2	140.1	43.5	65.5	97.8	44.6
Case C3	105.7	57.1	60	98.2	40.9
Case C4	81.7	73.0	54.5	98.5	37.3

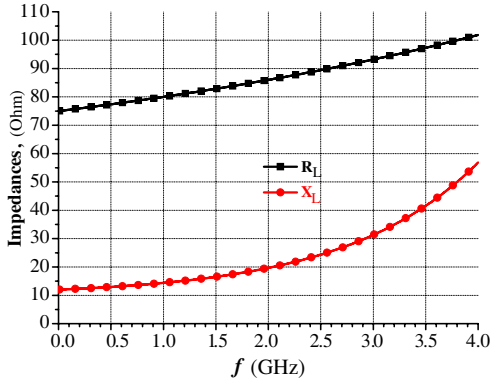

Figure 2. The parameters of the real and imaginary parts for frequency-dependent load impedance.

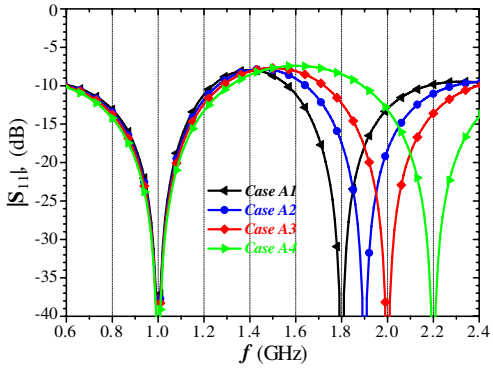

Figure 3. The input-port scattering parameters of the cases A1–A4.

amplifiers and power dividers. For experimental verifications, two microstrip generalized T-junction power dividers are constructed, designed, fabricated, and measured.

The circuit configuration of the generalized T-junction power divider is depicted in Figure 6. Since different power-dividing ratio performance at two different operating frequencies is required when the port-terminated impedances at three ports are the same and equal to Z_o, the input impedances Z_{ina} and Z_{inb} feature frequency-dependent values. It is assumed that the power-dividing ratio coefficients ($|S_{31}| / |S_{21}|$) at the first frequency f_1 and the second frequency f_2 are k_1 and k_2, respectively. Moreover, the ideal matching at f_1 and f_2 should be satisfied simultaneously. The values of the input impedances Z_{ina} and Z_{inb} can be derived from the dual-band matching

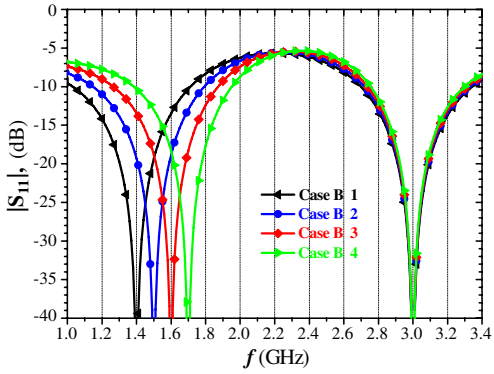

Figure 4. The input-port scattering parameters of the cases B1–B4.

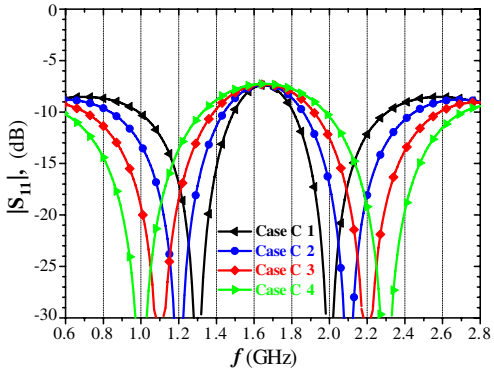

Figure 5. The input-port scattering parameters of the cases C1–C4.

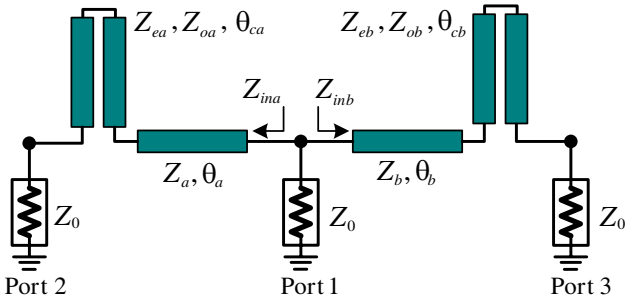

Figure 6. A generalized T-junction power divider including two proposed impedance transformers with $Z_0 = 50\,\Omega$.

Table 7. The designed circuit parameters of the two prototype generalized T-junction power dividers (Examples A and B).

Unit for impedances: Ω Unit for electrical lengths: Degree	**Example A** $f_1 = 0.4\,\text{GHz}$ $f_2 = 1\,\text{GHz}$ $k_1 = -1\,\text{dB}$ $k_2 = -3\,\text{dB}$	**Example B** $f_1 = 0.4\,\text{GHz}$ $f_2 = 1.02\,\text{GHz}$ $k_1 = 0\,\text{dB}$ $k_2 = -2\,\text{dB}$
Z_{ina} *at* f_1	89.7164	100
Z_{ina} *at* f_2	75.0594	81.5479
Z_{inb} *at* f_1	112.9463	100
Z_{inb} *at* f_2	149.7631	129.2447
Z_{ea}	93.9722	95.8902
Z_{oa}	46.5747	50.7191
θ_{ca} *at* f_1	51.4286	50.7042
Z_a	82.0613	90.3039
θ_a *at* f_1	25.7143	25.3521
Z_{eb}	86.2384	78.1739
Z_{ob}	70.1178	67.9978
θ_{cb} *at* f_1	51.4286	50.7042
Z_b	130.0584	113.6858
θ_b *at* f_1	25.7143	25.3521

and transmission requirements as

$$\begin{cases} Z_{ina} \text{ at } f_1 = \left(1 + k_1^2\right) R_S \\ Z_{ina} \text{ at } f_2 = \left(1 + k_2^2\right) R_S \end{cases}, \tag{12a}$$

$$\begin{cases} Z_{inb} \text{ at } f_1 = \frac{\left(1+k_1^2\right)}{k_1^2} R_S \\ Z_{inb} \text{ at } f_2 = \frac{\left(1+k_2^2\right)}{k_2^2} R_S \end{cases}. \tag{12b}$$

In the calculation process, the values of n in (4) and the sign of "$\pm$" in (9) should be chosen manually, as discussed in the Section 2. In the following two power divider examples the sign "+" is chosen for the Equation (9). Moreover, the situations $n = 0$ and $n = 1$ are considered in the analytical design procedures of the impedance transformers used for the ports 2 and 3, respectively. The calculated circuit parameters for Examples A and B are listed in Table 7.

A practical substrate with a relative dielectric constant of 3.48 and a height of 0.762 mm is applied to implement the designed Examples A and B. A representative layout of the prototype T-junction power divider is illustrated in Figure 7. The dimensions (unit: millimeters) of the Example A (B) are $w_m = 1.72(1.72)$, $w_{ma} = 0.69(0.55)$, $w_{mb} = 0.20(0.30)$, $w_{ca} = 0.87(0.81)$, $w_{cb} = 0.76(0.87)$, $l_{ma} = 34(33)$, $l_{mb} = 34(33)$, $l_{ca} = 67(66)$, $l_{cb} = 67(66)$, $s_{ca} = 0.17(0.23)$, and $s_{cb} = 1.10(1.50)$. Without any full-wave simulation optimizations, the layouts of the power dividers are fabricated directly using PCB technology. Figure 8 shows the photograph of the manufactured power dividers including Examples A and B. The smallest gap size

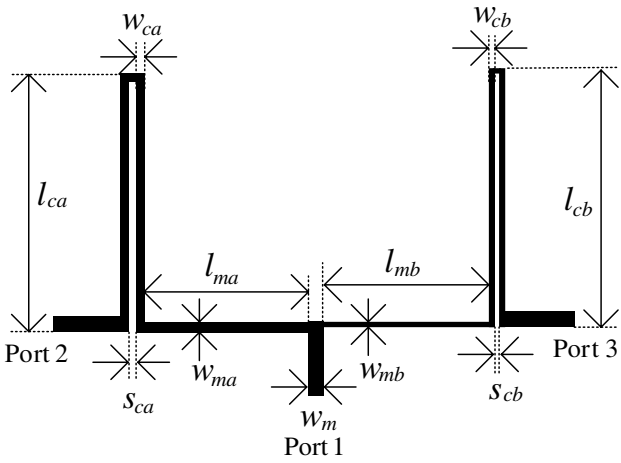

Figure 7. Typical layout of the generalized T-junction power divider using the proposed impedance transformers.

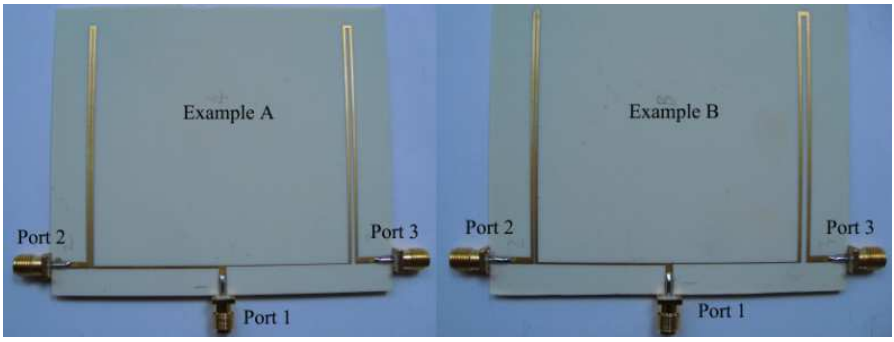

Figure 8. Photograph of the fabricated T-junction power dividers (Examples A and B) including two proposed impedance transformers.

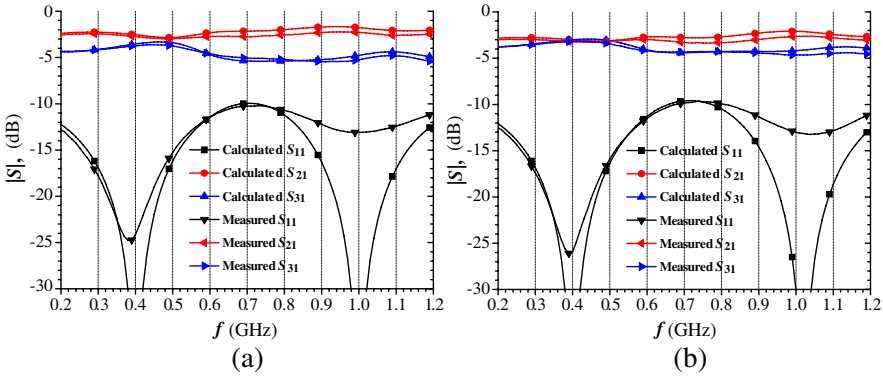

Figure 9. Photograph of the fabricated T-junction power dividers including two proposed impedance transformers. (a) Example A, and (b) Example B.

of the coupled-line section is approximately 0.17 mm, which can be implemented using conventional microstrip technology.

Two prototype power dividers are tested with Network Analyzer (Model: Agilent N5230C). The calculated scattering parameters are based on lossless coupled-line and transmission-line models, are not achieved from full-wave electromagnetic simulation tools. Figure 9 shows the frequency responses of the examples A and B. From scattering parameters of example A shown in Figure 9(a), it can be achieved that the measured $|S_{21}|$ and $|S_{31}|$ results are -2.72 dB and -3.73 dB at 400 MHz (-2.29 dB and -5.23 dB at 1 GHz), and these are very close to the calculated results of the ideal schematic circuit models, which are -2.54 dB and -3.54 dB at 400 MHz (-1.76 dB and -4.76 dB at 1 GHz). Similarly, the measured $|S_{21}|$ and $|S_{31}|$ results for the example B, as shown in Figure 9(b), are -3.22 dB and -3.19 dB at 400 MHz (-2.62 dB and -4.66 dB at 1.02 GHz), and these are very close to the calculated results of the ideal schematic circuit models, which are -3.01 dB and -3.01 dB at 400 MHz (-2.12 dB and -4.12 dB at 1.02 GHz). The minimum reflection coefficients within the first band around f_1 and the second band around f_2 for example A (example B) are -25 dB (-26 dB) and -13.1 dB (-13.2 dB), respectively. Note that the input matching parameters at the second frequency in examples A and B may be due to the unequal even- and odd-mode velocities in microstrip coupled lines and the inaccurate manufacturing quality of the PCB technology. The transmission losses, which occur in the measured $|S_{21}|$ and $|S_{31}|$ results, could be because the conductor loss, dielectric loss, radiation loss, discontinuous, and measurement errors.

5. CONCLUSION

A novel planar coupled-line dual-band impedance transformer which is suitable for frequency-dependent load impedances has been proposed in this paper. This transformer has the advantages of small size in simple circuit configuration, wide bandwidth, simple analytical design method, and easy planar implementation. The mathematical design formula is developed in simple analytical form, which provides a straightforward synthesis approach. A total of 12 cases have been used to theoretically verify the proposed circuit structure and its corresponding design method. Finally, for experimental verification and convenient measurement, two prototype microstrip T-junction power dividers with different power-dividing ratios at two different operating frequencies are designed, constructed, fabricated, and measured. Good agreement between the measured results and the calculated results verifies this novel transformer structure and the simple closed-form design equations. It can be believed that this dual-band coupled-line impedance transformer is useful for designing dual-band passive components and active components including dual-band Doherty power amplifiers.

ACKNOWLEDGMENT

This work was fully supported by a grant from City University of Hong Kong (Project No. 7002709) and supported in part by the National Natural Science Foundation of China (No. 61201027), the Fundamental Research Funds for Central Universities (No. 2012RC0301), and Open Project of the State Key Laboratory of Millimeter Waves (Grant No. K201316).

REFERENCES

1. Bahl, I. J., "Broadband and compact impedance transformers for microwave circuits," *IEEE Microwave Magazine*, Vol. 7, No. 4, 56–62, Aug. 2006.
2. Li, S., B. Tang, Y. Liu, S. Li, C. Yu, and Y. Wu, "Miniaturized dual-band matching technique based on coupled-line transformer for dual-band power amplifiers design," *Progress In Electromagnetics Research*, Vol. 131, 195–210, 2012.
3. Liu, Y., Y.-J. Zhao, and Y. Zhou, "Lumped dual-frequency impedance transformers for frequency-dependent complex loads," *Progress In Electromagnetics Research*, Vol. 126, 121–138, 2012.

4. Shamaileh, K. A. A., A. M. Qaroot, and N. I. Dib, "Non-uniform transmission line transformers and their application in the design of compact multi-band bagley power dividers with harmonics suppression," *Progress In Electromagnetics Research*, Vol. 113, 269–284, 2011.
5. Zhang B., Y.-Z. Xiong, L. Wang, S. Hu, and L.-W. Li, "3D transformer design by through silicon via technology and its application for circuit design," *Journal of Electromagnetic Waves and Applications*, Vol. 25, Nos. 17–18, 2513–2521, Jan. 2011.
6. Wu, B., C.-H. Liang, T. Su, and X. Lai, "Wideband coaxial filters with impedance matching for VHF/UHF diplexer design," *Journal of Electromagnetic Waves and Applications*, Vol. 22, No. 1, 131–142, Jan. 2008.
7. Monzon, C., "A small dual-frequency transformer in two sections," *IEEE Trans. Microw. Theory Tech.*, Vol. 51, No. 4, 1157–1161, Apr. 2003.
8. Wu, Y., Y. Liu, and S. Li, "A dual-frequency transformer for complex impedances with two unequal sections," *IEEE Microw. Wireless Compon. Lett.*, Vol. 19, No. 2, 77–79, Feb. 2009.
9. Liu, X., Y. Liu, S. Li, F. Wu, and Y. Wu, "A three-section dual-band transformer for frequency-dependent complex load impedance," *IEEE Microw. Wireless Compon. Lett.*, Vol. 19, No. 10, 611–613, Oct. 2009.
10. Chuang, M.-L., "Dual-band impedance transformer using two-section shunt stubs," *IEEE Trans. Microw. Theory Tech.*, Vol. 58, No. 5, Part 1, 1257–1263, May 2010.
11. Wu, Y., Y. Liu, S. Li, C. Yu, and X. Liu, "A generalized dual-frequency transformer for two arbitrary complex frequency-dependent impedances," *IEEE Microw. Wireless Compon. Lett.*, Vol. 19, No. 12, 792–794, Dec. 2009.
12. Nikravan, M. A. and Z. Atlasbaf, "T-section dual-band impedance transformer for frequency-dependent complex impedance loads," *Electronics Letters*, Vol. 47, No. 9, 551–553, Apr. 2011.
13. Ang, K. S., C. H. Lee, and Y. C. Leong, "A broad-band quarter-wavelength impedance transformer with three reflection zeros within passband," *IEEE Trans. Microw. Theory Tech.*, Vol. 52, No. 12, 2640–2644, Dec. 2004.
14. Jensen, T., V. Zhurbenko, V. Krozer, and P. Meincke, "Coupled transmission lines as impedance transformer," *IEEE Trans. Microw. Theory Tech.*, Vol. 55, No. 12, 2957–2965, Dec. 2007.
15. Wincza, K. and S. Gruszczynski, "Asymmetric coupled-line

directional couplers as impedance transformers in balanced and n-way power amplifiers," *IEEE Trans. Microw. Theory Tech.*, Vol. 59, No. 7, 1803–1810, Jul. 2011.

16. Chen, W., S. A. Bassam, et al., "Design and linearization of concurrent dual-band Doherty power amplifier with frequency-dependent power ranges," *IEEE Trans. Microw. Theory Tech.*, Vol. 59, No. 10, Part 1, 2537–2546, Oct. 2011.
17. Bassam, S. A., W. Chen, et al., "Linearization of concurrent dual-band power amplifier based on 2D-DPD technique," *IEEE Microw. Wireless Compon. Lett.*, Vol. 21, No. 12, 685–687, Dec. 2011.
18. Rawat, K., M. S. Hashmi, and F. M. Ghannouchi, "Double the band and optimize," *IEEE Microwave Magazine*, Vol. 13, No. 2, 69–82, Mar. 2012.
19. Rawat, K., M. S. Hashmi, and F. M. Ghannouchi, "Dual-band RF circuits and components for multi-standard software defined radios," *IEEE Circuits and Systems Magazine*, Vol. 12, No. 1, 12–32, First Quarter 2012.
20. Mongia, R., I. Bahl, and P. Bhartia, *RF and Microwave Coupled-Line Circuits*, Chapter 4, Artech House Publishers, Boston, 1999.